Continuous-Time Time-Stretched Analog-to-Digital Converter Array Implemented Using Virtual Time Gating

Yan Han, *Member, IEEE,* and Bahram Jalali, *Fellow, IEEE*

***Abstract*—We demonstrate the continuous-time operation of a time-stretch analog-to-digital converter array. A continuous-time RF signal is segmented into parallel channels and each channel is stretched in time prior to digitization. The technique offers improvement in the effective input bandwidth and sampling rate of the digitizer. The implementation uses virtual time gating for interleaving segments of the continuous-time RF signal. The signal is first modulated onto a linearly chirped optical carrier and then sliced, in time, using passive optical filters. This technique obviates the need for fast switching gates. It results in minimum interchannel mismatch and in hardware efficiency since all channels are stretched using the same electro-optic modulator and the same dispersive elements.**

***Index Terms*—Analog-to-digital conversion (ADC), channel mismatch, microwave photonics, optical signal processing, time stretch.**

I. Introduction

THE proliferation of digital signal processing in communication and radar systems has placed an ever increasing burden on the analog-to-digital converter (ADC). Consequently, the ADC is the performance bottleneck in many advanced systems. Time-stretch preprocessing has been proposed as a means to enhance the effective sampling rate and input bandwidth of ADCs [1], [2]. Depicted in Fig. 1(a), a time-stretch analog preprocessor with a stretch factor of M confers an M-fold increase in effective bandwidth and sampling rate. Presently, the preprocessing is best accomplished using time-wavelength transformation techniques performed in the optical domain. This is mainly due to the availability of low-loss and wide-band optical dispersive elements, such as a single mode fiber. As shown in Fig. 1(b), a nearly transform-limited ultra-short broad-band pulse, generated by the so-called SuperContinuum (SC) source [3] is first chirped by propagation through a dispersive fiber. The electrical signal modulates the intensity of this linearly chirped optical carrier using an electro-optic modulator. When propagating through the second dispersive fiber, the modulated signal is stretched when the chirp pulse is broadened. A slowed down version of the input electrical signal is obtained after photodetection.

Using this configuration, 480 GSa/s time-stretched ADC with 96-GHz intrinsic bandwidth has been previously demonstrated, where an effective number of bits of 5.17 was measured over a 9.6-GHz passband (PB) centered at a 26 GHz carrier [4]. Time aperture and 3 dB analog bandwidth are crucial parameters in time-stretch system. Optical dispersion, used to stretch the waveform, also limits the RF bandwidth. This occurs due to destructive interference between the frequency mixing terms of the upper and lower modulation sidebands of the optical carrier. Single-sideband modulation has been proposed and demonstrated as a possible solution to extend the analog bandwidth [5], [6]. An alternative technique using phase diversity has also been proposed and demonstrated to eliminate this bandwidth limitation [4]. To achieve a long aperture time, large values of dispersion over large optical bandwidths are required. Dispersion compensating fiber (DCF) is chosen as the dispersive medium as it offers a high dispersion coefficient $(D = 90\ \mathrm{ps/km/nm})$ to loss (0.6 dB/km) ratio. Assuming an optical bandwidth of 20 nm, 10 ns time aperture can be achieved with a concomitant loss of approximately 3 dB. This time aperture corresponds to a frequency resolution of 100 MHz. To obtain a larger time aperture or finer frequency resolution, a larger optical bandwidth can be used. However, a larger optical bandwidth exposes other issues such as spectral flatness of optical source and the optical amplifier, and the wavelength dependence of the electro-optic modulator [7]. It is clear that other means for extending the time aperture are necessary.

A time-stretch system operating in continuous time can eliminate the time-aperture limitation. This can be achieved using the architecture shown in Fig. 2 which uses the spatial dimension to stretch a continuous-time signal without loss of information. The continuous input signal is segmented and interleaved into four parallel channels. The duty cycle in each parallel channel is now 25% allowing the waveform to be stretched by a maximum of four times. After being captured by slow ADCs, the original waveform is obtained by concatenating the segments in the digital domain. This architecture is somewhat similar to traditional time-interleaved ADCs where a high speed signal is sampled by a parallel array of sequentially clocked digitizers [8]. The main difference is that in the time-stretch system, the ADCs see the slowed down signal and the sampling in each channel is above the Nyquist rate. By contrast, ADCs see the full bandwidth of the incoming signal in the traditional architecture, and sampling

Manuscript received May 30, 2004; revised September 27, 2004 and January 4, 2005. This work was supported by the Defense Advanced Research Project Agency (DARPA) under the Photonic Analog-to-Digital Converter (PACT) Program. This paper was recommended by Associate Editor A. Wang.

Y. Han is with College of Optics and Photonics: CREOL and FPCE, University of Central Florida, Orlando, FL 32816 USA (e-mail: yanhan@creol.ucf.edu).

B. Jalali is with Optoelectronic Circuits and Systems Laboratory, Department of Electrical Engineering, University of California, Los Angeles, CA 90095-1594 USA (e-mail: jalali@ucla.edu).

Digital Object Identifier 10.1109/TCSI.2005.851674

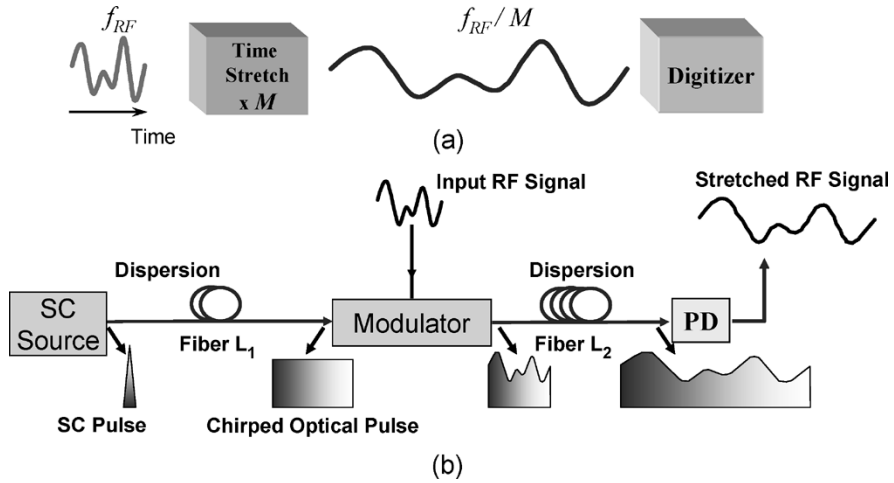

Fig. 1. (a) Conceptual block diagram of time-stretched ADC. (b) Schematic diagram of the photonic implementation of time stretch.

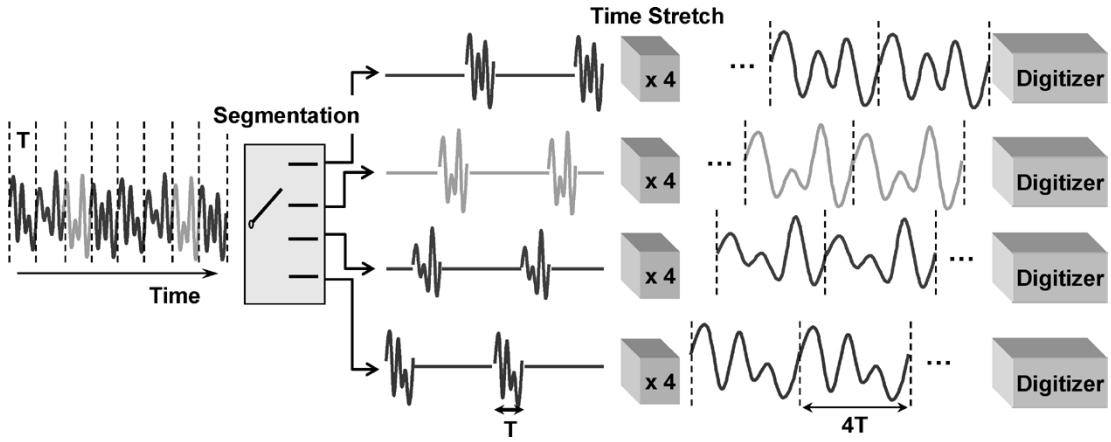

Fig. 2. Conceptual diagram of continuous-time stretched ADC.

by each time-interleaved digitizer is done at a fraction of the Nyquist rate. This fundamental advantage can be exploited in estimating and correcting for the interchannel mismatch errors in the time-stretch ADC system [9].

The continuous-time stretched ADCs rely on a means to segment-interleave the incoming signal. The use of an active gating switch is the most obvious approach. However, the time–wavelength mapping offers a clever way to do this. The gating can be performed using a passive optical filter. An additional advantage is the ability to stretch all channels (segments) in a single dispersive fiber, hence saving hardware and avoiding interchannel mismatches caused by different pieces of fiber not being identical.

A simple information capacity argument can be used to illustrate the lack of information loss in the time-stretch system of Fig. 2. Assuming that the incoming signal has a bandwidth of B, perturbed by additive white Gaussian noise of power spectral density $N_0/2$, the information capacity is $C = B\log_2(1 + (P/N_0B))$ where P is the average signal power. In the time-stretch system, the continuous signal is segmented into M channels and stretched by M times. Time stretch reduces the signal bandwidth and as hence each subchannel has B/M bandwidth. In addition, after stretching the power of each channel is reduced to P/M, due to energy conservation. The information capacity of each channel is now $(B/M)\log_2(1 + ((P/M)/N_0(B/M))) = C/M$. For the M channel system, the capacity is $M \cdot (C/M) = C$. Hence, the information capacity is the same before and after time stretch.

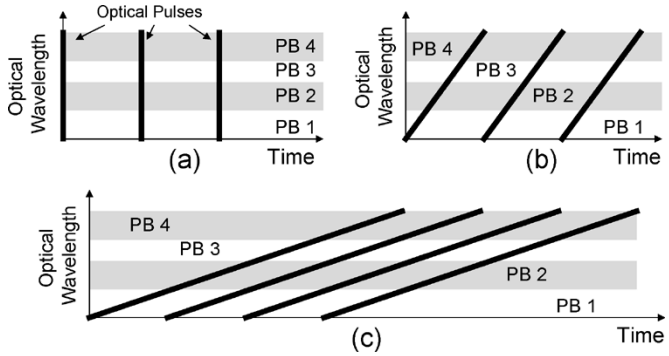

Fig. 3. Virtual time-gating principle.

In this paper, the continuous-time operation of a time-stretched ADC is demonstrated for the first time. The proof-of-concept demonstration exploits a novel time-wavelength gating technique to perform the signal segmentation.

II. Principle of Virtual Time Gating

In this section, we describe how the time-gating function described in Fig. 2 can be accomplished without the use of an electronic switch or demultiplexer. The principle of virtual time gating is shown in Fig. 3 and it greatly simplifies the

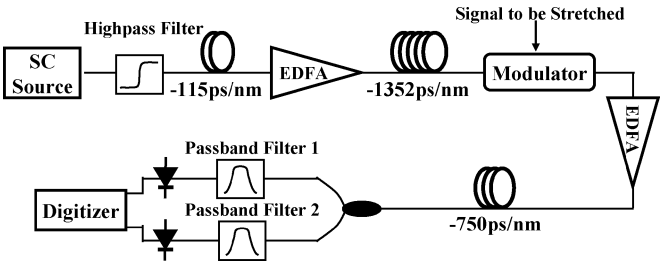

Fig. 4. Experiment setup for a two-channel continuous-time stretch ADC. SC: Supercontinuum. EDFA: Erbium-Doped Fiber Amplifier. Highpass filter: 1570 nm above. PB filter 1: 1576 nm with 20-nm bandwidth. PB filter 2: 1594 nm with 20-nm bandwidth.

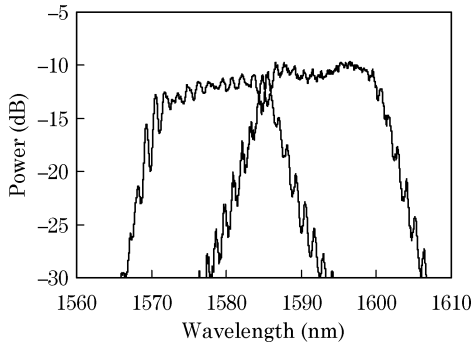

Fig. 5. Optical spectrum of two channels used in the continuous-time stretch experiment.

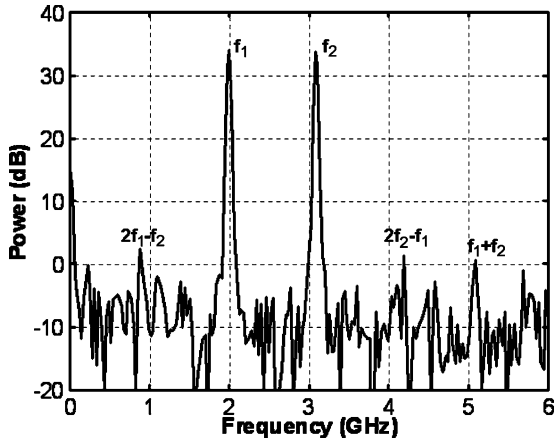

Fig. 6. Measured digital magnitude spectrum using two-tone test.

implementation of continuous-time stretch ADC. To illustrate the process, a two-dimensional time-wavelength representation is used. Fig. 3(a) shows a pulse train consisting of ultra-short broad-band optical pulses. For clarity, the optical spectrum is divided into four PBs. After propagation through the first dispersive elements, pulses are linearly chirped and broadened in time by an amount equal to the inter-pulse spacing [Fig. 3(b)]. Following modulation of the electrical signal onto this waveform (not shown), the waveform is dispersed again leading to time-dilation [Fig. 3(c)]. Since the electrical signal is superimposed onto the optical carrier, it is also stretched in the process. At this point, there is significant temporal overlap (cross-talk) between adjacent segments. Fortuitously, however, the segments that overlap in time are separated in optical wavelength. This permits their separation using a passive optical filter that carves the spectrum into individual optical PBs. Because of the linear time-wavelength mapping, the spectrum carving is equivalent to temporal gating. In other words, each optical PB corresponds to a distinct time-segment.

An important feature of the virtual time gating is that temporal segmentation of the electrical signal is performed using a passive optical filter and without the need for an electronic switch or demultiplexer. Another important feature is a single electro-optic modulator and a single set of dispersive elements are used for all channels. This avoids interchannel mismatch problems and offers hardware simplicity. Again, the resulting overlap in time can be tolerated because of separation in optical wavelength. This time-wavelength gating scheme is adopted in the experiment described in Section III.

III. Continuous–Time Stretch Experiments

A two-channel continuous-time stretch experiment that uses the virtual time gating scheme is shown in Fig. 4. Broad-band optical pulses are created using a supercontinuum generation process described elsewhere [3]. A highpass filter (1570 nm above) is used to select the long wavelength portion of the spectrum. This portion has higher signal-to-noise ratio since it is away from the 1530–1560-nm range, where amplified spontaneous emission (ASE) noises of the optical amplifier in SC source reside. The so-obtained nearly transform-limited pulses propagate through a length L_1 DCF with total dispersion $D_1L_1 = -1467$ ps/nm dispersion. An optical amplifier is inserted in the middle of fiber to compensate for fiber propagation loss. The location is chosen to minimize the detrimental effect of optical nonlinearities in the fiber, while maintaining a good signal-to-noise ratio. The chirped pulse is modulated by electrical signal in a Mach–Zehnder modulator. The modulated pulse then propagates through a length, L_2, of DCF with $D_2L_2 = -750$ ps/nm dispersion to stretch the modulation. The stretch factor is $1 + D_2L_2/D_1L_1 = 1.5$ [1]. At the end of fiber, a 3-dB coupler is used to split two channels and each channel is filtered by a PB optical filter. The two $\sim$20-nm PBs are centered at 1576 nm and 1594 nm. We note that this configuration is not ideal because of the splitting loss of the 3-dB coupler. To eliminate the splitting loss, which would be required in a system with large number of channels, a coarse wavelength division multiplexing (WDM) filter would be used. The two channels are subsequently photodetected and digitized concurrently, by two inputs of Tektronix real-time oscilloscope TDS7404 (4 GHz input bandwidth and 10 GSa/s per channel). In principle, the digitizer and the SC source must be synchronized, although this was not implemented in the present experiments since the TDS7404 does not provide external synchronization. The distortion caused by the nonuniform spectrum of the chirped pulse is suppressed using the digital filtering technique described in [2]. We note that the two channels are stretched in the same piece of fiber and are not separated until the digitization step. Also, the time gating is performed using passive optical filters eliminating the need for electronic switches.

The optical spectrum of two adjacent channels obtained without any RF modulation is shown in Fig. 5. Optical filters used in the system have finite PB ripples that are clearly visible in the spectrum. The slow variations in the spectrum are due to the spectral shape of the broad-band pulse and the gain profile

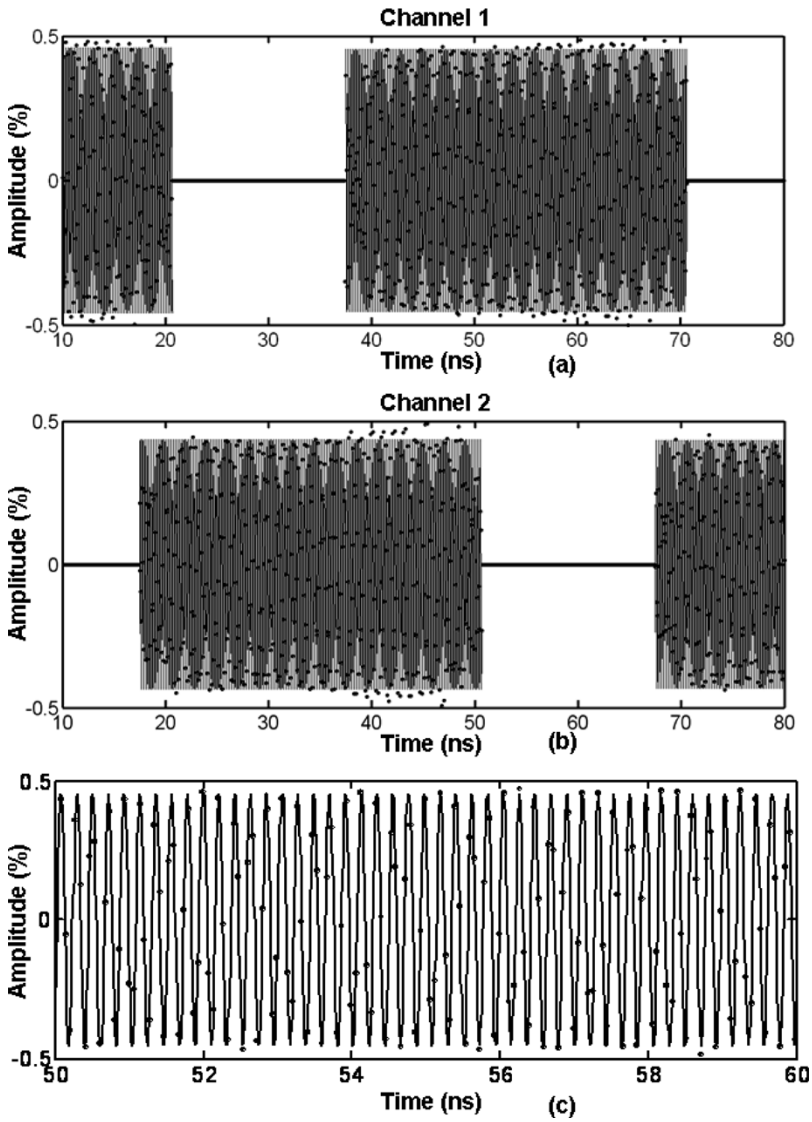

Fig. 7. Measured 4.7-GHz signal after interleaving. The symbols are sample points and the line is the fitted sine curve. (a) Channel 1 at 1576 nm. (b) Channel 2 at 1594 nm. (c) Portion of (a).

of the optical amplifier. Both the ripples and the slow variations can be removed using simple signal processing performed in the digital domain [2]. The finite roll-off of filter PBs, causing overlap between adjacent segments is clearly visible. In the two-channel system, the maximum possible stretch factor is two. Because of the finite roll-off, the stretch factor cannot reach the maximum value, and was chosen to be $\sim$1.5 in the present experiment. Interestingly, the overlap between adjacent segments creates redundancy that can be used to estimate the interchannel mismatch. This feature is described later.

The signal quality after time stretching is evaluated using the two-tone test. Both 2- and 3.1-GHz signals are combined before the modulator. Each segment is subsequently stretched, digitized, and recorded. The magnitude spectrum of one segment is shown in Fig. 6, obtained using discrete fourier transform (DFT). A Hanning window is applied to limit the frequency leakage due to the finite window length. This also gives a larger weight to the center of each segment, where the signal-to-noise ratio is highest. The resulting spectrum shows the stretched tones with more than 30-dB spurious-free dynamic range (SFDR). Intermodulation tones corresponding to the second- and third-order distortion are marked. The third-order distortion is due to the nonlinear transfer function of the MZ modulator which imposes a limit on the dynamic range given by $\mathrm{SFDR} = -20\log(m^2/8) = 34\,\mathrm{dB}$, where $m = 0.4$ is the optical modulation index of each tone (defined as half the peak-to-peak optical power divided by the average). The second-order distortion is due to the dispersion in the fiber which distorts the phase balance between modulation sidebands and generates frequency-dependent second-order nonlinearity [2]. Broad-band linearization techniques in the form of post distortion performed in the digital domain can potentially be useful.

The virtual time gating concept is clearly demonstrated in Fig. 7 which shows a captured 4.7-GHz tone. The tone is slowed down to $4.7/1.5 = 3.13$ GHz, allowing it to be captured by the 4-GHz digitizer. The continuous-time signal is passively interleaved into two channels using two optical filters. In the experiment, a clock skew exists between the two channels due to the propagation length mismatch after the 3-dB coupler. This is calibrated by measuring the propagation delay with oscillo-

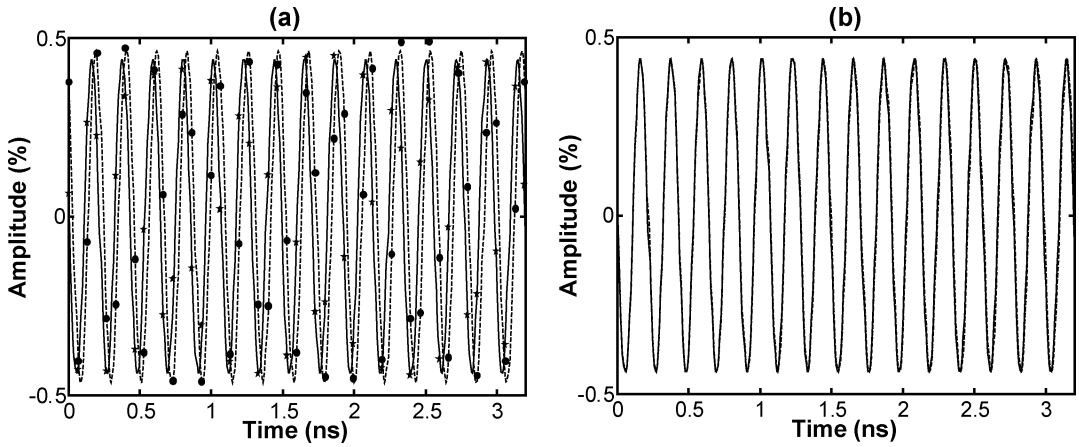

Fig. 8. Overlap between two adjacent channels. The star and circular symbols represent the sample points of two channels, respectively. The solid and dashed lines are the fitted curves. (a) Precalibration where gain and time mismatches are visible. (b) Postcalibration.

scope using the 1-ps pulse laser. The calibration accuracy is equal to the minimum resolution of oscilloscope (∼50 ps). The overlap between two channels corresponds to the overlap in the spectrum shown in Fig. 5 and can be used to estimate interchannel mismatches. The slight amplitude variation across the time window is caused by the nonlinear group velocity dispersion (dependence of D on wavelength) of the fiber [2]. Qualitatively, the DCF fiber has a higher D at the longer wavelength (corresponding to the start of each segment). A higher D induces a larger dispersion-induced power penalty at high frequencies.

A well-known problem in ADC array is the interchannel mismatch. This is the major limiting factor in the conventional sample-interleaved ADCs [8], [10]. Similarly, channel mismatches limit the proposed time-stretched ADC array and a thorough theoretical analysis is given in [11]. The overlap section for two adjacent channels is shown in Fig. 8(a) where gain mismatch and clock skew are clearly visible. The digital filtering technique used to correct for the spectral nonuniformity remove the dc component; hence no dc offset is present. The gain mismatch and clock skew generate spurious tones and deteriorate the system dynamic range. A fundamental difference between the time-stretched ADC array and the conventional sample-interleaved system is that in the former, each channel samples the signal at or above the Nyquist rate. This is a unique feature enabled by time stretching and can be exploited to estimate the mismatch errors. The so-called adaptive online calibration technique was numerically studied in [9]. If $S_1(k)$ and $S_2(k)$ represent the DFT of samples in the overlapped section between adjacent segments, the dc mismatch a, gain mismatch b, and clock skew r can be calculated as [9]

$$
\begin{aligned}
a &\cong \left[\frac{\sum_{k=1}^{W-1}|S_2(k)|^2}{\sum_{k=1}^{W-1}|S_1(k)|^2}\right]^{\frac{1}{2}} \\
b &\cong \frac{[|S_2(0)| - a\,|S_1(0)|]}{W} \\
r &\cong \frac{W}{2\pi}\frac{\Delta}{\Delta k}\left[\angle S_2(k) - \angle S_1(k)\right] \qquad (1)
\end{aligned}
$$

where r is normalized to the sample interval, and W is the number of sample points in the overlapped section. $\angle$ denotes the phase angle, and $\Delta/\Delta k$ operator takes the slope of its argument. Fig. 8(b) shows the overlapped sections after correction using the estimated gain mismatch and clock skew obtained from (1). The estimated gain mismatch was 1.05 and the clock skew (relative to the sample interval) was −0.398. Because the error is obtained from the signal itself for each optical pulse, not from a test-signal, one is able to perform real-time error correction, addressing amplitude and frequency dependencies and dynamic variations of the error.

As demonstrated, the mismatches between optical PB channels can be corrected using the above algorithm. Within each channel, the accuracy between segments need be examined as well. Since each segment in a channel corresponds to an optical pulse of source laser, the quality of signal in a channel is mainly decided by the pulse laser stability, which has been improved over years. Taking digitization into consideration, the laser repetition frequency must be phase-locked to the clock of digitizer. The lack of phase locking will cause clock walk-off between segments in a channel. In this experiment, the lack of external synchronization function of the digitizer and laser prevents evaluating the ADC performance over a long time aperture.

IV. Discussion

Virtual time gating greatly simplifies the implementation of a continuous-time stretch ADC array by passively gating the signal and stretching all channels using a single optical modulator and a single dispersive element. On the other hand, this technique increases the optical bandwidth that is required, since the optical bandwidth available for each channel is the total optical bandwidth divided by the number of channels, M. A more bandwidth-efficient system would use an $1:M$ electrical demultiplexing switch before the time-stretch processor. In this case optical bandwidth of each channel is equal to the total optical bandwidth of the system. However, this architecture would require M modulators and M dispersive elements resulting in higher system complexity and more severe interchannel mismatch problems.

The stretch factor of time-stretch system is $1 + D_2/D_1$, where D_1 and D_2 are the dispersion coefficients of fiber 1 and fiber 2. One may expect that a nonlinear group velocity dispersion (wavelength-dependent D) will cause a nonuniform stretch factor and hence distort the signal. Specifically, the stretch factor will be different along the linearly chirped supercontinuum pulse and hence between adjacent time segments. It has been shown that when the two fibers have matched dispersion characteristics, the stretch factor is $1 + L_2/L_1$, independent of the higher order dispersion [2]. In the experiments, however, a slight mismatch exists between the two fibers resulting in a frequency difference of $\sim$0.3% between two adjacent segments. The effect is more pronounced when a larger optical bandwidth is used. Hence, it is more severe in a continuous-time time-stretched ADC array that makes use of the virtual time gating.

V. Summary

In summary, we have demonstrated a two-channel time-stretch ADC array. To achieve continuous-time operation, the implementation uses virtual time gating where a continuous-time analog signal is segmented in time, using passive optical filters. All channels in the ADC array share the same optical source, electro-optic modulator and dispersive elements, resulting in hardware efficiency and minimum interchannel mismatch. Online mismatch correction, a unique feature of time-stretch architecture which removes the remaining mismatch due to optical filters and photodetectors, is experimentally demonstrated.

References

[1] F. Coppinger, A. S. Bhushan, and B. Jalali, "Photonic time stretch and its application to analog-to-digital conversion," *IEEE Trans. Microw. Theory Tech.*, vol. 47, no. 7, pp. 1309–1314, Jul. 1999.

[2] Y. Han and B. Jalali, "Photonic time-stretched analog-to-digital converter: fundamental concepts and practical considerations," *J. Lightw. Technol.*, vol. 21, no. 12, pp. 3085–3103, Dec. 2003.

[3] O. Boyraz, J. Kim, M. N. Islam, F. Coppinger, and B. Jalali, "Broadband, high-brightness 10-Gbit/s supercontinuum source for A/D conversion," in *Proc. Lasers and Electro-Optics Conf. (CLEO'00)*, May 7–12, 2000, pp. 489–490.

[4] Y. Han, O. Boyraz, and B. Jalali, "Ultrawide-bond photonic time-stretch A/D converter employing phase diversity," *IEEE Trans. Microw. Theory Tech.*, vol. 53, no. 4, pp. 1404–1408, Apr. 2005.

[5] J. M. Fuster, D. Novak, A. Nirmalathas, and J. Marti, "Single-sideband modulation in photonic time-stretch analogue-to-digital conversion," *Electron. Lett.*, vol. 37, no. 1, pp. 67–68, Jan. 2001.

[6] Y. Han and B. Jalali, "Time-bandwidth product of the photonic time-stretched analog-to-digital converter," *IEEE Trans. Microw. Theory Tech.*, vol. 51, no. 7, pp. 1886–1892, Jul. 2003.

[7] S. Dubovitsky, W. H. Steier, S. Yegnanarayanan, and B. Jalali, "Analysis and improvement of Mach–Zehnder modulator linearity performance for chirped and tunable optical carriers," *J. Lightw. Technol.*, vol. 20, no. 5, pp. 886–891, May 2002.

[8] W. C. Black and D. A. Hodges, "Time interleaved converter arrays," *IEEE J. Solid-State Circuits*, vol. SC-15, no. 12, pp. 1022–1029, Dec. 1980.

[9] Y. Han, B. Rezaei, V. P. Roychowdhury, and B. Jalali, "Adaptive online calibration in time stretched ADC arrays," in *Proc. Instrumentation and Measurement Technology Conf.*, vol. 2, May 20–22, 2003, pp. 1212–1216.

[10] Y. C. Jenq, "Digital spectra of nonuniformly sampled signals: fundamentals and high-speed waveform digitzers," *IEEE Trans. Instrum. Meas.*, vol. 37, no. 2, pp. 245–251, Jun. 1988.

[11] B. Asuri, Y. Han, and B. Jalali, "Time-stretched ADC arrays," *IEEE Trans. Circuits Syst. II, Analog Digit. Signal Process.*, vol. 49, no. 7, pp. 521–524, Jul. 2002.

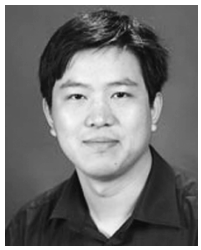

Yan Han (M'04) received the B.S. and M.S. degrees in electronic engineering from Tsinghua University, Beijing, China, and the Ph.D. degree in electrical engineering from the University of California, Los Angeles, in 1998, 2000, and 2004, respectively.

He is currently with the College of Optics and Photonics (CREOL and FPCE), University of Central Florida, Orlando,. His research interests include the areas of time-wavelength signal processing, advanced modulation formats for optical communications, microwave photonics, and nonlinear optics.

Bahram Jalali (M'89–SM'97–F'04) is a Professor of Electrical Engineering, the Director of the Defense Advanced Research Project Agency (DARPA) Center for Optical Analog–Digital System Technology (COAST), and the Director of the Optoelectronic Circuits and System Laboratory at the University of California at Los Angeles (UCLA). From 1988 to 1992, he was a Member of Technical Staff at the Physics Research Division, AT&T Bell Laboratories, Murray Hill, NJ, where he conducted research on ultrafast electronics and optoelectronics. While on leave from UCLA from 1999 to 2001, he founded Cognet Microsystems, a Los Angeles based fiber-optic component company. He served as Cognet's CEO, President, and Chairman, from the company's inception through its acquisition by Intel Corporation, in April 2001. From 2001 to 2004, he served as a Consultant at Intel Corporation. His current research interests are in microwave photonics, integrated optics, and fiber optic integrated circuits. He has over 200 publications and holds 6 U.S. patents.

Dr. Jalali is a Fellow of Optical Society of America (OSA) and the Chair of the Los Angeles Chapter of the IEEE Lasers and Electro Optics Society (LEOS). He was the General Chair for the IEEE International Conference on Microwave Photonics (MWP) in 2001 and its Steering Committee Chair from 2001 to 2004. He is a member of the California Nano Systems Institute (CNSI). He currently serves on the Board of Trustees of the California Science Center. He has received the BridgeGate 20 Award for his contribution to the southern California economy.